Time-Resolved X-Ray Line Diagnostics of Laser-Produced Plasmas*

UCRL-87422-Rev. 1

Robert L. Kauffman, Dennis L. Matthews

University of California
Lawrence Livermore National Laboratory
Livermore, CA 94550

UCRL--87422-Rev.1

DE83 005575

and

J. D. Kilkenny, R. W. Lee

Blackett Laboratory, Imperial College,
London, England**

Abstract

We have examined the underdense plasma conditions of laser irradiated disks using K x-rays from highly ionized ions. A 900 ps laser pulse of 0.532 μm light is used to irradiate various Z disks which have been doped with low concentrations of tracer materials. The tracers, whose Z's range from 13 to 22, are chosen so that their K x-ray spectrum is sensitive to typical underdense plasma temperatures and densities. Spectra are measured using a time-resolved crystal spectrograph recording the time history of the x-ray spectrum. A spatially-resolved, time-integrated crystal spectrograph also monitors the x-ray lines. Large differences in Al spectra are observed when the host plasma is changed from SiO_2 to PbO or In. Spectra will be presented along with preliminary analysis of the data.

*Work performed under the auspices of the U.S. Department of Energy by Lawrence Livermore National Laboratory under contract #W-7405-ENG-48.

**Work partially supported by NATO Research Grant #292.81.

DISCLAIMER

This report was prepared as an account of work sponsored by an agency of the United States Government. Neither the United States Government nor any agency thereof, nor any of their employees, makes any warranty, express or implied, or assumes any legal liability or responsibility for the accuracy, completeness, or usefulness of any information, apparatus, product, or process disclosed, or represents that its use would not infringe privately owned rights. Reference herein to any specific commercial product, process, or service by trade name, trademark, manufacturer, or otherwise, does not necessarily constitute or imply its endorsement, recommendation, or favoring by the United States Government or any agency thereof. The views and opinions of authors expressed herein do not necessarily state or reflect those of the United States Government or any agency thereof.

DISTRIBUTION OF THIS DOCUMENT IS UNLIMITED

Discussion

We have performed a series of measurements to investigate the usefulness of x-ray line intensities as electron density and temperature diagnostics. Line intensities from highly stripped ions have been used successfully in diagnosing high temperature astrophysical and magnetically confined plasmas[1,2]. Line intensities of He-like and H-like species from laser-produced plasmas have also been used by various researchers to estimate electron temperature and densities in the coronal plasma region[3]. In general, these measurements have been compromised due to the relatively dense, transient nature of laser-produced plasmas. Large temperature and density gradients also complicate the analysis in determining a unique temperature and density. In our experiment we have begun studying these effects to assess their importance for predicting temperature and densities of underdense plasmas.

The experiments were performed in the single beam interaction chamber at the Center Laser Facility of Rutherford Laboratory[4]. A single beam of 0.532 μm light is focussed using an f/1 lens onto planar targets of various Z materials. The average intensity on target is $\sim 10^{15}$ W/cm^2. The target normal is tilted 10° with respect to the beam. The targets are discs of CH, SiO_2 and high Z materials which have been doped with low concentrations of elements whose lines are to be used as diagnostics. Typically, the dopant levels are less than ten atomic percent; although for some high Z targets larger concentrations are needed. In all cases the dopant levels should not change significantly the Z or hydrodynamics of the plasma.

Two crystal spectrographs measure the x-ray spectra. A spectrograph located at 80° to the disc normal measures the time-integrated spectra. A 50 μm slit placed in front of the spectrograph spatially resolves the plasma along the incident beam direction. An example of the data is shown in Fig. 1. In general, line emission extends away from the absorption region characterized by high continuum emission into the coronal region

where only line emission is observed. An x-ray crystal streak camera located on the opposite side of the target time resolves the line emission with 80 psec resolution[5]. Figure 2 shows an example of the data. For the lower Z targets the x-ray line emission lasts significantly longer than the continuum emission. For the high Z targets the x-ray lines tend to follow the laser pulse.

The data from both instruments are analyzed deriving intensities for the various x-ray lines. Examples of the time-integrated data for Si doped in CH and PbO targets are shown in Figures 3 and 4. Similar spectra were also obtained with the time-resolved spectrograph.

The model to calculate the line ratios used in the study is a straight forward steady state level population model. The inputs require the temperature, density, and all the appropriate rate constants of interest. In the present case we include all of the ground states up to the Be-like stage and then have excited states as well as ground state for Li-, He-, and H-like ions. In the case of the Li-like and He-like we also include the autoionizing states which form satellites on the resonance transition of the next ion stage.

The rates of primary interest; i.e., the ionization rates, the electron collision rates in the He-like ground to n equals 2 complex, and the collision rates between the autoionizing state are found in the following references:

Ionization Rates	Lotz Sampson Sampson & Golden	Z. Physics 280 466 (69) (e.g.) J. Physics B 13, 2645, (80)
Collision Rates in He-like	Vinogradov et al	Soc. J. Quant. El., 5, 630 (75)
Collisions between Autoionizing Li-like	Blaha, Jacobs	Phys. Rev. A 21 525 (80)
Like and He-Like	Goett, et al	Atom. Data & Nuc. Data, 25, 185 (80)

With these rates and standard calculations of the remaining rates, which are less crucial, one can produce the ratios given. The one outstanding problem is to resolve whether the plasma does reach the steady state and for this we ran the problem time dependent using a Lagrangian fluid element as a "test particle" and found that the ions easily come to a steady state when reasonable plasma expansion was used.

Examples of the various ratios are shown in Figures 5-8. These have been chosen since they are sensitive primarily to a single parameter, either N_e or T_e, and not both simultaneously. Experimental values of Si line ratios from doped CH and PbO are indicated. The results are summarized in Table I. The two targets produce similar results indicating that the plasma parameters are similar in the line emitting region.

The different line ratios do not give a unique plasma temperature and density. The most striking disagreements are with line ratios from different charge states. The He-like resonance to Li-like line indicates a lower T_e than the Lyman to He-like resonance ratio. This may be due to the spatial gradient along the laser beam. Even though the spectrum is spatially-resolved it is averaged over about 50 μm so that large gradients may exist. We plan to use hydrodynamic code predictions coupled with the line ratio code to investigate this effect. We are also investigating ionization equilibrium and their effects on the line ratios.

An example of the time-resolved data is shown in Fig. 9. The line ratio of the Si Lyα and He-like $2\,^1P_1$ line is plotted as a function of time. The time history of the lines are very similar for the two cases.

Finally, various dopants have been seeded into CH targets and their x-ray spectra have been measured. The $^1P_1/^3P_1$ line ratios are plotted in the Figure 10 comparing with predicted line ratios from Boiko et al.[8]. For the seed targets the line ratios indicate emission is from near critical density implying the seeds are sampling the same region of the target.

References

1. A. H. Gabriel and C. Jordan, Astrophys. J. 186, 327 (1973).

2. C. De Michelis and M. Mattioli, Nuclear Fusion 21, 677-754 (1981); and references therein.

3. N. J. Peacock, in Laser-Plasma Interactions, edited by R. A. Cairns and J. J. Sanderson (Scottish Universities Summer School in Physics, Edinburgh, Scotland, 1980) pp. 711-806; and references therein.

4. Central Laser Facility Annual Report, 1981, Rutherford and Appleton Laboratories, RL-81-040 (unpublished).

5. C. L. S. Lewis, M. J. Lamb, J. D. Kilkenny, S. Keats, and M. H. Key, Central Laser Facility Annual Report, 1980, Rutherford Laboratory, RL-80-026 (unpublished) pp. 6.1-6.2.

6. M. Galanti and N. J. Peacock, J. Phys. B 8, 2427-2447 (1975).

7. V. A. Boiko, S. A. Pikuz, and A. Ya. Faenov, J. Phys. B 12, 1889-1909 (1979).

DISCLAIMER

This document was prepared as an account of work sponsored by an agency of the United States Government. Neither the United States Government nor the University of California nor any of their employees, makes any warranty, express or implied, or assumes any legal liability or responsibility for the accuracy, completeness, or usefulness of any information, apparatus, product, or process disclosed, or represents that its use would not infringe privately owned rights. Reference herein to any specific commercial products, process, or service by trade name, trademark, manufacturer, or otherwise, does not necessarily constitute or imply its endorsement, recommendation, or favoring by the United States Government or the University of California. The views and opinions of authors expressed herein do not necessarily state or reflect those of the United States Government thereof, and shall not be used for advertising or product endorsement purposes.

TABLE I

Summary of Plasma Parameters from Si Line Intensities

	N_e (cm^{-3})	
	CH	PbO
$\frac{2^1P_1}{2^3P_1}$	1×10^{20}	1.1×10^{20}
$\frac{3^1P_1}{2^3P_1}$	1×10^{20}	1×10^{20}
$\frac{2^3P_1 + Si^{+11}(MN+ST)}{Si^{+11}(ABCD+JKL+QR)}$	$0.3 - 1.1 \times 10^{21}$	$2 - 8 \times 10^{20}$

	Te(keV)	
	CH	PbO
$\frac{Ly\alpha}{2^1P_1}$	0.83	0.83
$\frac{Ly\beta}{3^1P_1}$	0.85	1.05
$\frac{2^1P_1}{Si^{+11}(ABCD+JKL+QR)}$	0.40	0.53

0924I

EXAMPLE OF A SPACIALLY RESOLVED SPECTRUM FROM AN Al-DOPED GLASS TARGET

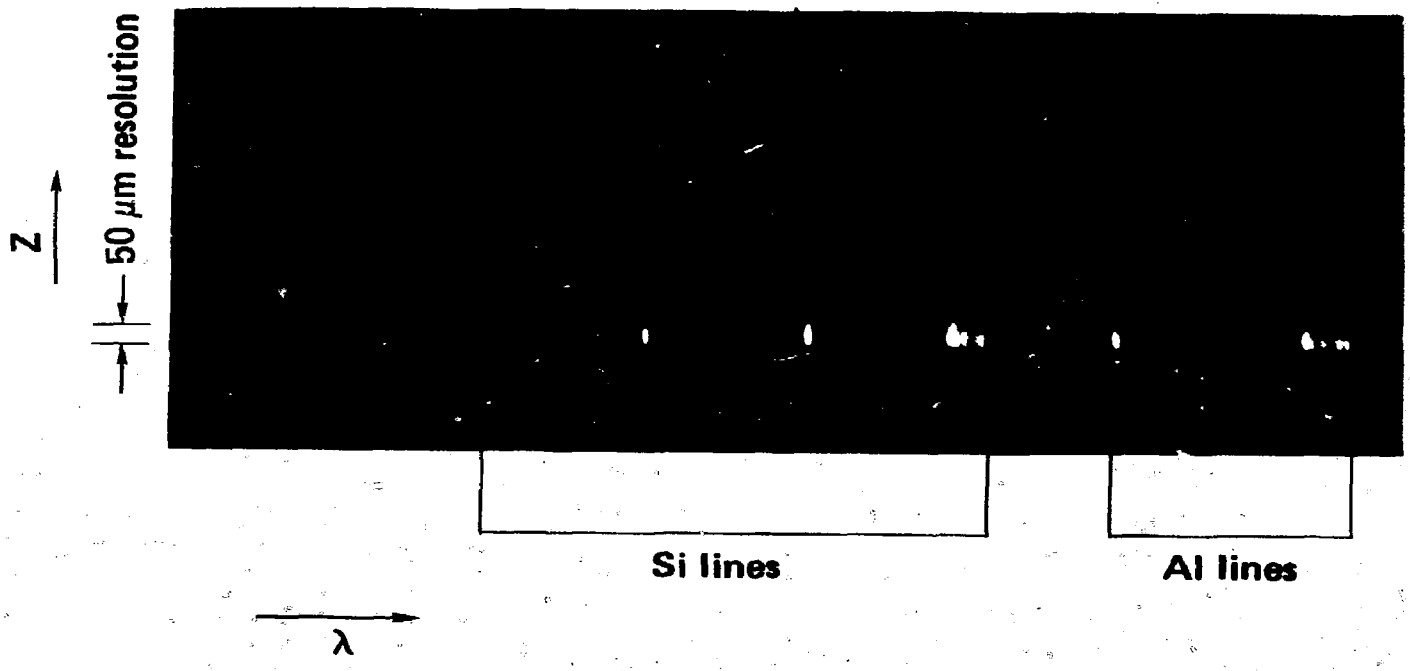

Figure 1

EXAMPLE OF A TIME-RESOLVED SPECTRUM FROM AN Al DOPED GLASS TARGET

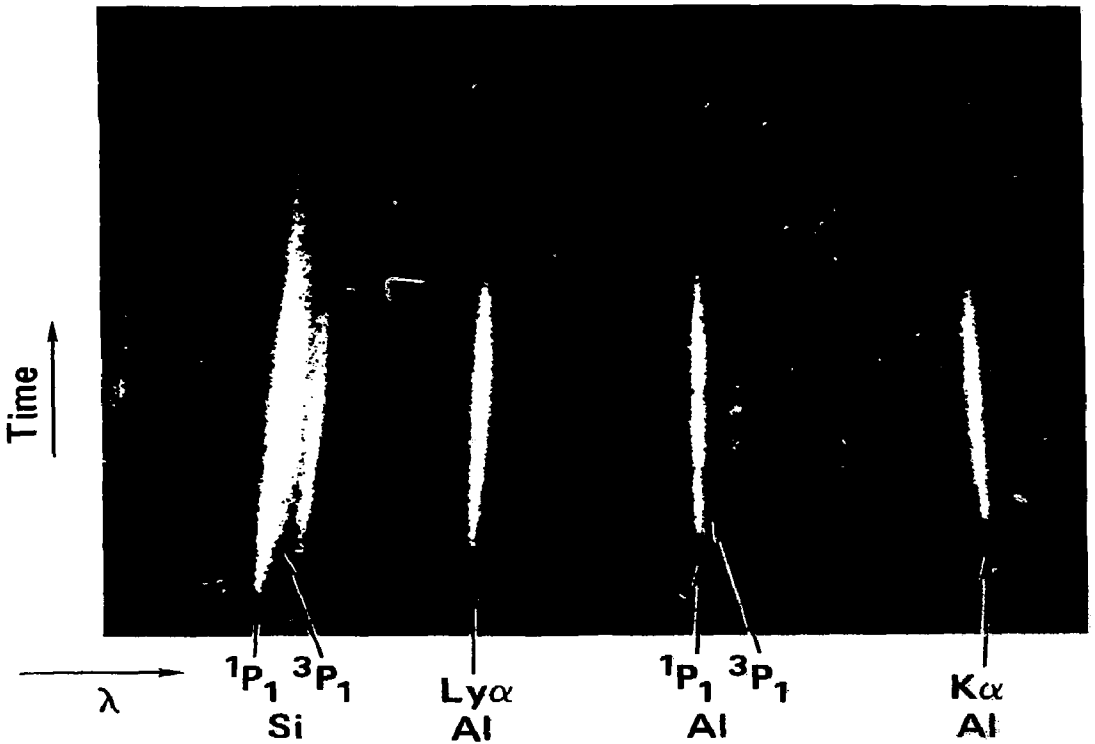

40-90-0482-1657

Shot 1/7/82 #27
10/82

Figure 2

X-RAY SPECTRUM FROM Si SEEDS IN A CH DISK TARGET

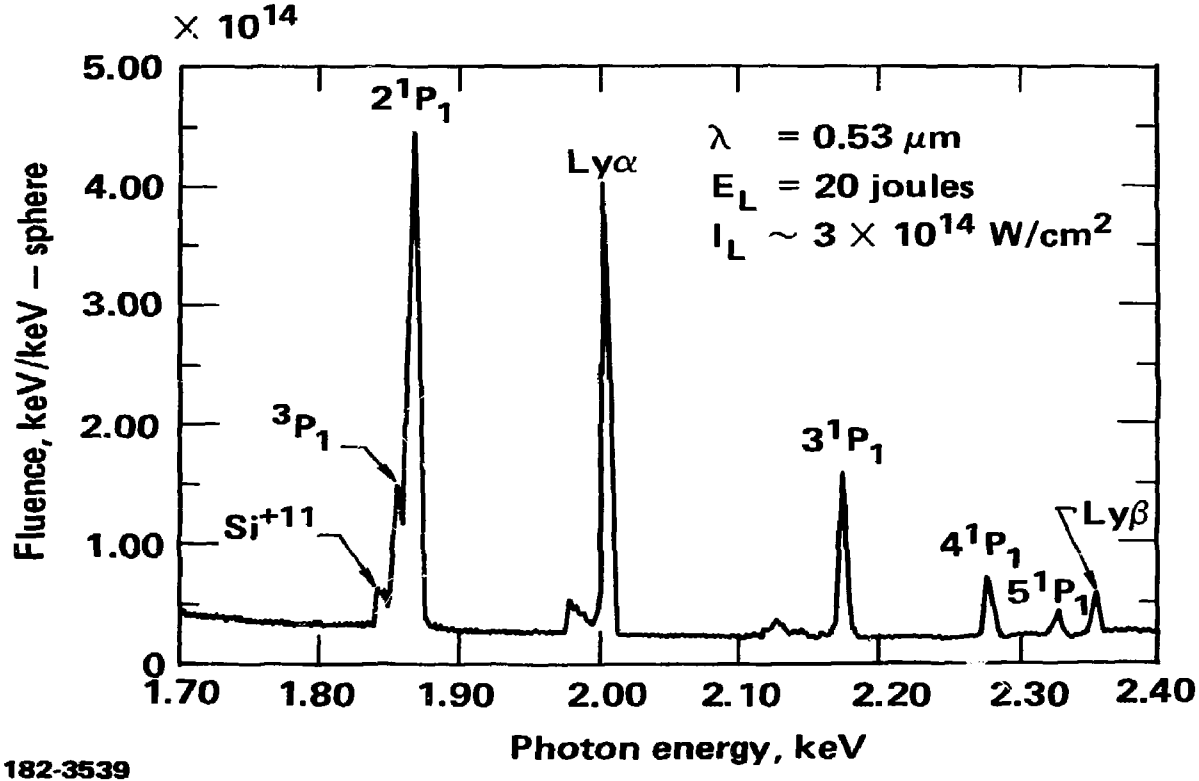

40-01-1182-3539

Figure 3

X-RAY SPECTRUM FROM Si IN A PbO DISK TARGET

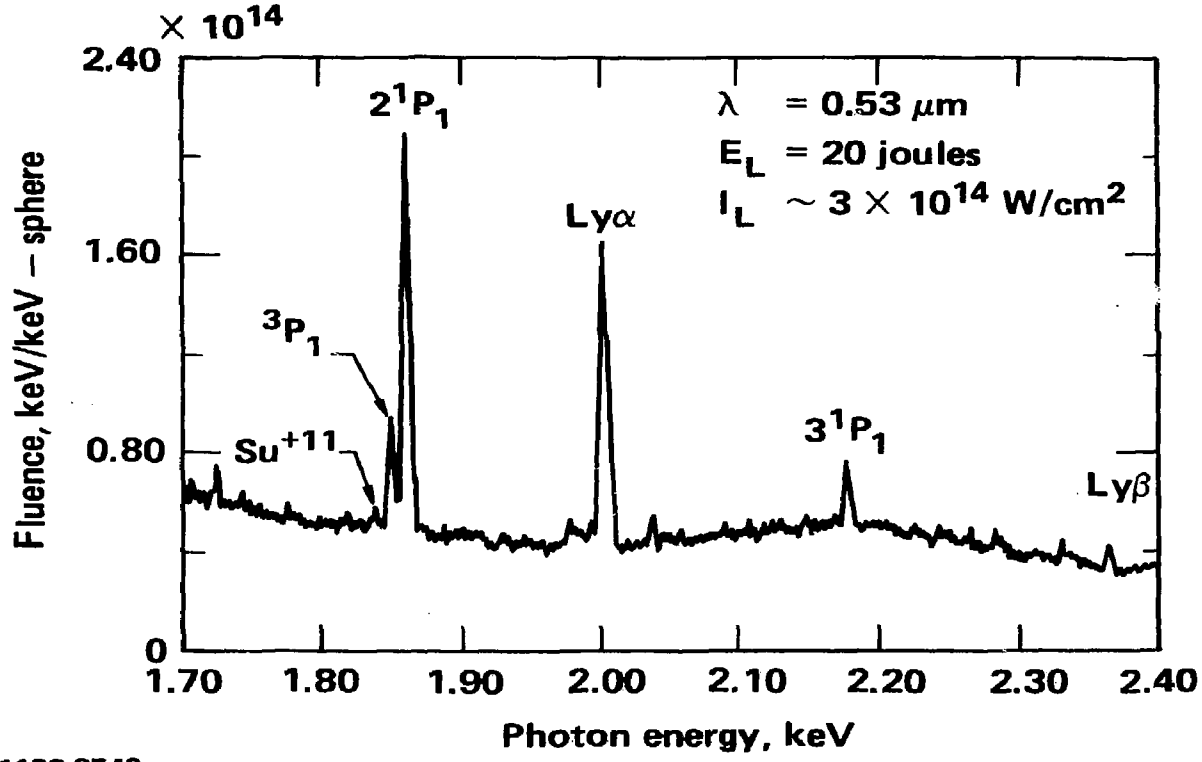

40-01-1182-3540

Figure 4

RATIO OF INTERCOMBINATION TO Li-LIKE SATELLITES IN Si CAN BE USED AS A DENSITY DIAGNOSTIC

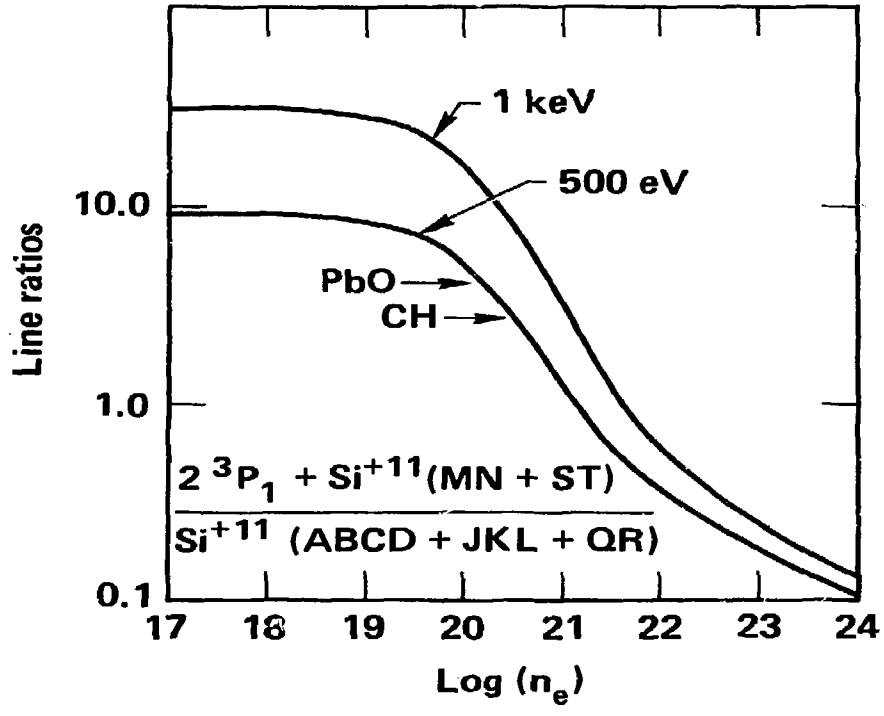

40-01-1082-3421

Figure 5

RATIO OF He-LIKE RESONANCE TO INTERCOMBINATION LINES IN Si CAN BE USED AS DENSITY DIAGNOSTICS

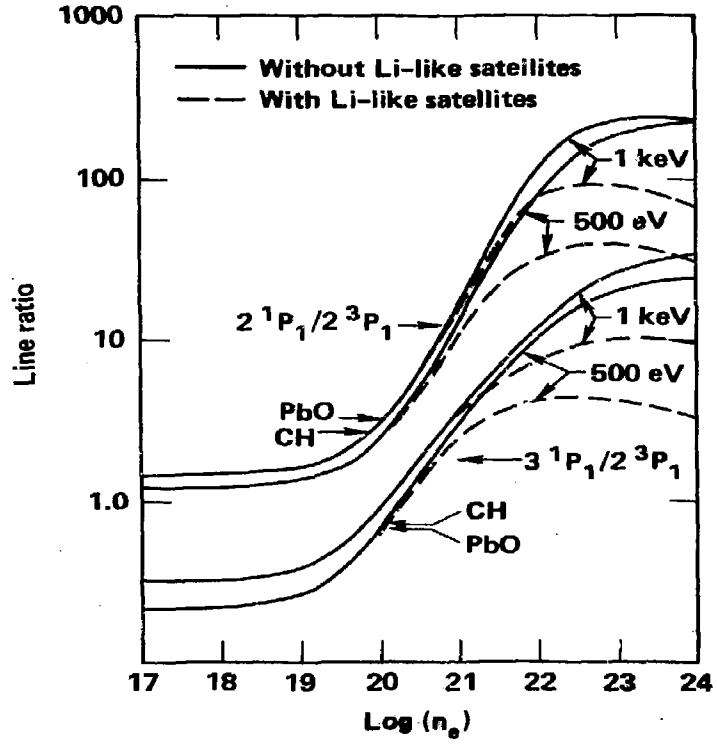

40-01-1082-3420

Figure 6

RATIOS OF LYMAN TO HE-LIKE LINES FROM Si CAN BE USED TO ESTIMATE THE LASER PLASMA CORONAL TEMPERATURES

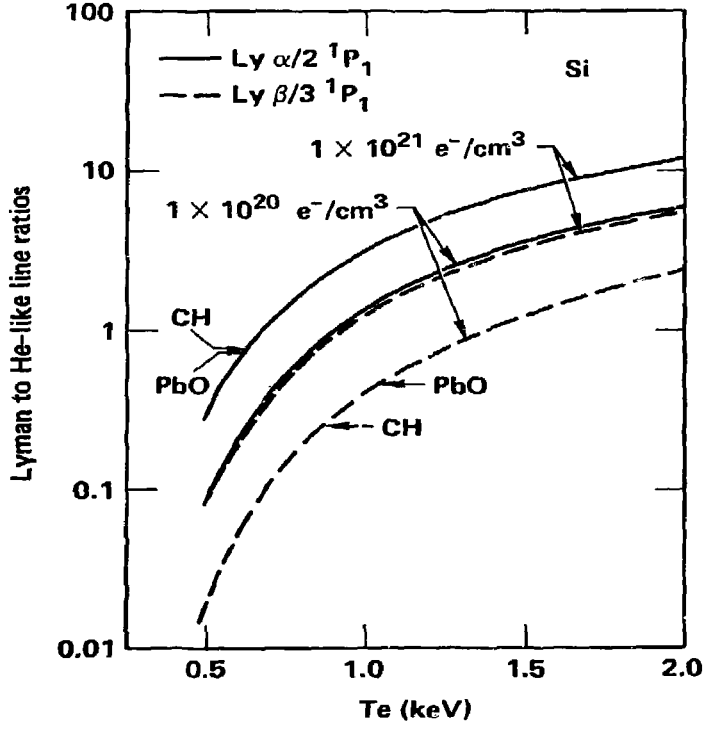

40-01-1082-3422

Figure 7

RATIO OF He-LIKE RESONANCE TO Li-LIKE SATELLITES IN Si CAN BE USED AS A CORONAL TEMPERATURE DIAGNOSTIC

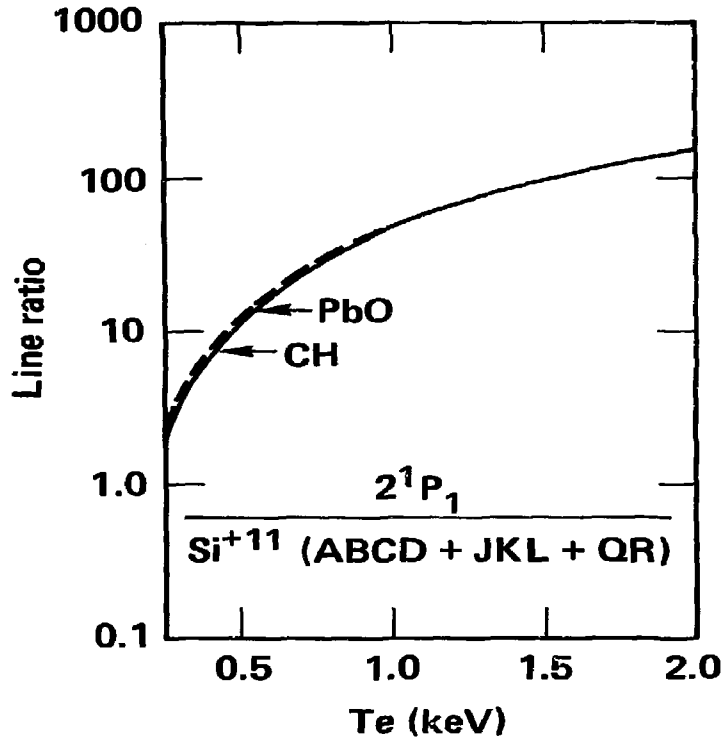

40-01-1082-3419

Figure 8

Si LINE RATIOS CAN BE USED TO DERIVE A TIME RESOLVED CORONAL TEMPERATURE

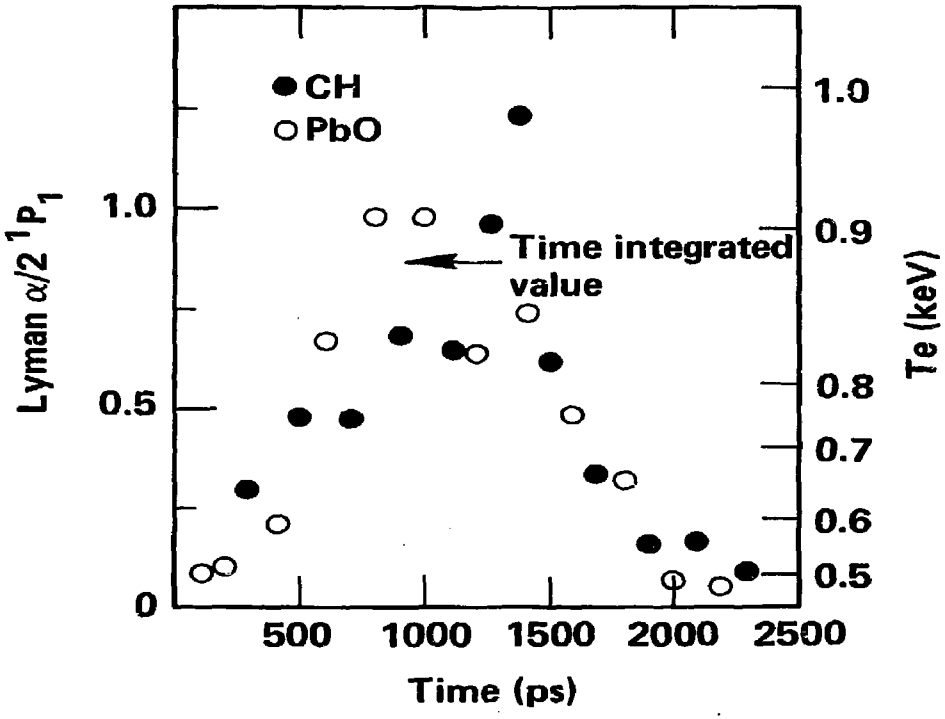

40-01-1082-3423

Figure 9

SIMPLE ANALYSIS OF $^1P_1/^3P_1$ RATIO SHOWS THAT DOPANT EMISSION IN CH OCCURS AROUND CRITICAL DENSITY FOR 0.532 nm LIGHT

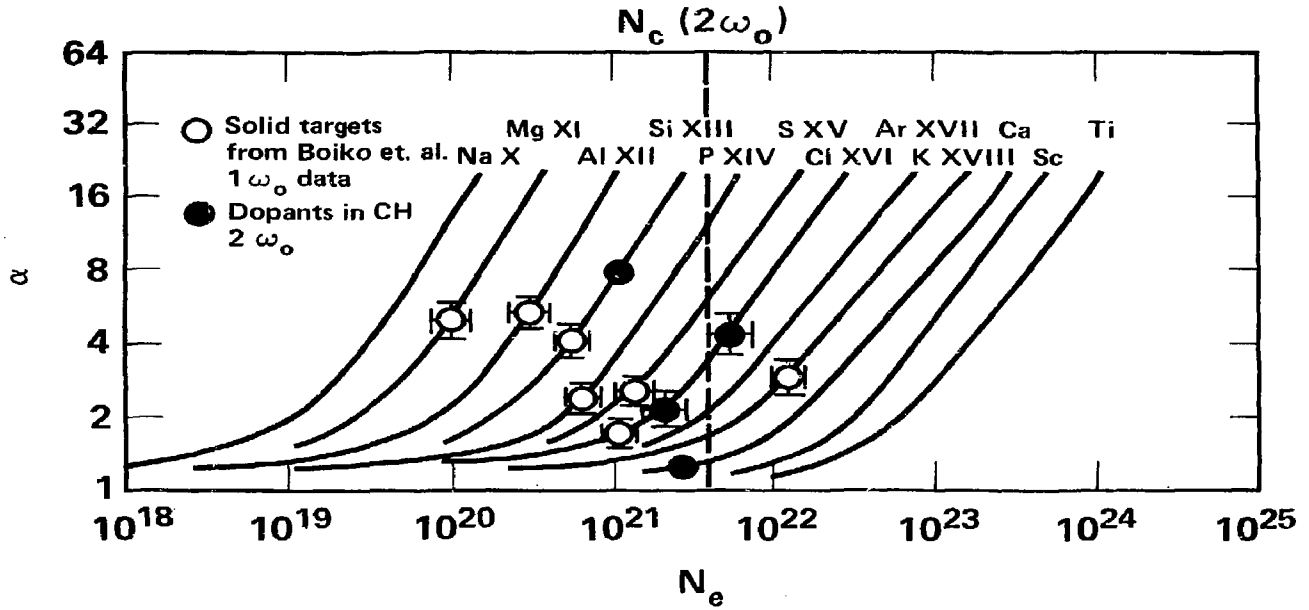

40-01-0582-1750

Figure 10